White Rose Research Online

eprints@whiterose.ac.uk
https://eprints.whiterose.ac.uk
Universities of Leeds, Sheffield and York

Deposited via The University of Sheffield.

White Rose Research Online URL for this paper:
https://eprints.whiterose.ac.uk/id/eprint/242676/

Version: Published Version

Article:
Zaki, M., Greco, G., Moreno-Tortolero, R.O. et al. (2026) A perspective on the evolution of artificial silk fibre research. Communications Materials, 7 (1). 159. ISSN: 2662-4443

https://doi.org/10.1038/s43246-026-01232-8

Reuse
This article is distributed under the terms of the Creative Commons Attribution (CC BY) licence. This licence allows you to distribute, remix, tweak, and build upon the work, even commercially, as long as you credit the authors for the original work. More information and the full terms of the licence here:
https://creativecommons.org/licenses/

Takedown
If you consider content in White Rose Research Online to be in breach of UK law, please notify us by emailing eprints@whiterose.ac.uk including the URL of the record and the reason for the withdrawal request.

UNIVERSITY OF LEEDS
University of Sheffield
UNIVERSITY of York

communications materials

A Nature Portfolio journal

Review article

https://doi.org/10.1038/s43246-026-01232-8

A perspective on the evolution of artificial silk fibre research

Check for updates

Martin Zaki [1] ✉, Gabriele Greco[2,3], Rafael O. Moreno-Tortolero[4,5], Chris Holland [6] & Benjamin J. Allardyce[1] ✉

For over a century, artificial silk spinning has pursued the exceptional mechanical performance of natural fibres, largely through a molecular-centric strategy. Limitations in artificial systems have been attributed to insufficient molecular weight, incomplete sequence architecture, or loss of native terminal domains, factors also thought to disrupt liquid-liquid phase separation (LLPS) and hierarchical assembly. LLPS is proposed to concentrate and pre-organise silk proteins, facilitating alignment during spinning and formation of hierarchical structures that underpin mechanical performance. Here, we reevaluate this paradigm through comparisons of regenerated silk fibroin (RSF), recombinant silk proteins, and regenerated undegummed silk (RUS). Advances across these systems have substantially narrowed the molecular gap with native silk, and under optimised conditions, all can produce fibres with comparable mechanical properties. While LLPS and hierarchical organisation can be induced in RSF and recombinant systems, these features do not consistently improve mechanics, suggesting native-like assembly alone is insufficient. RUS, which retains multicomponent interactions, most closely reflects the native system, yet still exhibits distinct rheology. Collectively, this indicates that artificial dopes lack compositional complexity and ability to respond to dynamic physiochemical gradients of the silk gland. Future progress in artificial spinning will require reconstructing the multicomponent, non-equilibrium environment governing silk assembly in nature.

Natural silk fibres represent one of the most sophisticated materials produced in nature, combining high strength and extensibility to generate what is arguably one of the toughest fibres known[1]. Unlike synthetic high-performance fibres, whose processing requires harsh solvents, high temperatures, or extreme pressures, silk is spun under precisely controlled aqueous, ambient conditions[2]. Its exceptional properties arise not merely from composition or molecular weight (MW), but from a tightly regulated spinning process where proteins are stored at very high concentrations as metastable aqueous solutions and undergo rapid, controlled denaturation and solidification in response to external biochemical and mechanical stresses[3,4].

Silk spinning, being a stress-induced phase separation, is an intrinsically non-equilibrium process, involving the precise application of mechanical work over defined timescales to reorganise protein hydrogen bonding and initiate hierarchical self-assembly spanning nanometre to micrometre length scales. Along the silk gland and spinning duct, gradients in ions and pH[5–10], progressive dehydration[11], confinement within narrowing channels[12], and evolving shear and extensional flow act synergistically with protein sequence to direct hierarchical assembly[13,14], from molecular conformations and nanofibrillar precursors to macroscopic fibres[15]. This multiscale organisation, underpinned by high fibroin MW, is likely to reinforce silk's mechanical performance[15–17]. Moreover, water and ions act not as passive solvents but as active regulators of protein interactions, phase behaviour and structural transitions, working in concert with applied flow deformation stress fields[2,4,18–20].

Beyond these gradients, growing evidence indicates that silk proteins at certain times and sections of the gland are organised via liquid-liquid phase separation (LLPS), enabling storage at high concentrations whilst suppressing aggregation[20,21]. This phase behaviour is thought to develop along the gland length in response to changes in pH, ions, hydration and flow, progressively biasing proteins toward adopting aligned, β-sheet-rich assemblies[22]. Importantly, these condensates are dynamic, varying across

[1]Deakin Institute for Frontier Materials, Deakin University, Geelong Waurn Ponds Campus, Geelong, VIC, Australia. [2]Department of Animal Biosciences, Swedish University of Agricultural Sciences, Uppsala, Sweden. [3]Department of Civil Engineering and Architecture, University of Pavia, Pavia, Italy. [4]School of Biochemistry and Biomedical Sciences, University of Bristol, Bristol, UK. [5]Max Planck-Bristol Centre for Minimal Biology, University of Bristol, Bristol, UK. [6]School of Chemical, Materials and Biological Engineering, Sir Robert Hadfield Building, University of Sheffield, Sheffield, UK. ✉e-mail: martin.zaki@deakin.edu.au; Ben.allardyce@deakin.edu.au

BOX 1 | definitions and terminology used for silk materials and assembly

Native silk—in solution, silk directly obtained from a silk gland, typically by dissection of the posterior section of the middle gland prior to spinning. In fibre form, silk is spun naturally by an organism.

RSF (regenerated silk fibroin)—silk solution produced by degumming native silk fibres to remove sericin and associated proteins, followed by dissolution of the purified fibroin. The resulting dope can be further processed into a range of material formats, including artificial spinning to produce fibres.

Recombinant silk—artificial silk proteins produced through heterologous expression of engineered silk gene constructs in host organisms (e.g. bacteria, yeast, plants or animals). The resulting dope can be further processed into a range of material formats, including artificial spinning to produce fibres.

RUS (regenerated undegummed silk—silk solution obtained by dissolving native silk fibres without prior degumming, thereby retaining fibroin, sericin and other native protein components. The resulting dope can be further processed into a range of material formats, including artificial spinning to produce fibres.

Native-like—a descriptor indicating partial resemblance to native silk in a specific attribute (e.g. molecular weight, terminal domain preservation, phase behaviour or mechanical performance), without implying full replication of the molecular architecture, compositional complexity or physicochemical environment of the native silk gland.

Hierarchical organisation—the presence of structural ordering across multiple length scales, spanning molecular conformations, secondary structure motifs and their assembly into nanofibrils, which further organise into micro- and macroscopic architectures.

development and cocoon construction stage, realising a structural 'anticipation' above that of an individual molecule[23]. While these insights are important for contextualising fibre formation in this review, they are not intended as a comprehensive evaluation of silk self-assembly, but rather to highlight key physicochemical features that influence spinning outcomes.

Since the earliest attempts to produce artificial silk, researchers have sought to decode and replicate this process ex vivo. While the importance of spinning conditions, such as pH[5,6,24], ions[7–9], dehydration[2], and flow has long been recognised[13,25], early artificial systems were fundamentally limited by compromised molecular integrity[26]. As a result, environmental variables could rarely be isolated or manipulated independently, and MW became the dominant, and often unavoidable, limiting factor[27,28]. Within this context, two strategies dominate: (i) dissolution of native silk followed by regeneration, and (ii) recombinant production of silk proteins in heterologous hosts (Box 1)[26]. While artificial fibre spinning inevitably departs from the biological system[28–30], this discussion focusses analysis on aqueous wet-spinning in an effort to preserve the biomimetic relevance to the natural spinning. Processing routes involving non-aqueous solvents, such as hexafluoroisopropanol (HFIP) or formic acid, are mostly excluded, as they depart fundamentally from the aquamelt nature of native silk dopes[2].

Likewise, individual studies vary widely in the production and storage of silk protein dopes, spinning parameters, including coagulant chemistry and pH, protein concentration, draw ratios and post-processing; therefore, it is difficult to compare outcomes directly across the literature[31]. Interpretation is further complicated by the lack of standardised mechanical testing protocols; variations in gauge length, strain rate, environmental conditions (temperature and humidity), how diameter is determined, and data analysis methods (engineering vs true stress–strain) can significantly influence reported fibre properties[31,32]. Together, this methodological heterogeneity obscures structure-property relationships and hampers rigorous cross-study comparison. To enable meaningful comparison, this perspective focuses primarily on MW and intact protein sequence as a unifying variable, unless otherwise specified. This constraint allows a simpler direct comparison between artificial systems and the native spinning process, helping to distinguish limitations that arise from molecular integrity from those imposed by the processing environment. Finally, we acknowledge that silk-producing organisms differ in gland anatomy, physiology and silk protein composition and fibroin amino acid sequence architecture (Box 1). However, the limited availability of systematic, within-species datasets spanning regenerated silk fibroin (RSF), recombinant and regenerated undegummed silk (RUS) processing necessitates cross-species comparisons where appropriate.

Early artificial systems failed to reproduce native spinning behaviour or fibre performance[26], with recent studies associating this primarily to molecular degradation, reduced MW, and loss of intact terminal domains[25,33]. In native silks, the termini act as pH and ion-responsive oligomerisation modules that mediate protein-protein association, which is thought to enable stability during storage and reduce the energetic threshold for fibre formation during spinning[4,33–36]. Consequently, and taken from lessons in polymer processing, restoring large, intact silk proteins above the threshold to ensure entanglement became an early priority[37,38]. Recent advances now meet these prerequisites: systems that preserve native-like MW[25,33,39,40], and native molecular architecture, including intact termini under aqueous conditions, recover key features of natural silk formation ex vivo, exhibiting native-like solution behaviour and nanofibrillar organisation, together with high toughness previously considered unattainable outside the organism[41,42]. These findings suggest that the long-standing MW and hierarchical assembly barriers have been substantially cleared[26]. Yet full convergence remains elusive, e.g. artificial fibres might exhibit lower molecular alignment than native cocoon silk[41], which in part is attributable to processing (Box 2)[43].

RSF: the molecular weight shortfall

RSF provided the first practical route to processing silk outside the organism and remains widely studied[26,44]. By dissolving native *Bombyx mori* (*B. mori*) silk fibres and reforming them into films[45], fibres[26], sponges[46], or gels[47], RSF enabled systematic investigation of silk's properties using polymer-processing frameworks.

RSF systems are fundamentally constrained by upstream processing steps designed for textiles rather than molecular preservation. The domestication of *B. mori* prioritised ease of reeling and reduced sericin content, rather than optimisation of mechanical performance[48,49]. Chief among these is degumming, which removes sericin using chemical, thermal, or enzymatic treatments[50–54]. While effective for textiles, degumming usually induces extensive fibroin hydrolysis[25,50,55], often cleaving both the repetitive core and terminal domains (Figs. 1, S1 and S2)[30,33]. Consequently, RSF exists as a spectrum of molecular integrity, with emerging methods approaching native-like states, though not yet fully equivalent. When RSF is in a degraded molecular state, characterised by significantly reduced and broadened molecular weight distributions relative to native silk, the damage is already embedded in the feedstock prior to regeneration, thereby limiting the attainable solution and fibre properties.

Within this paradigm, the inferior properties of wet-spun RSF fibres were therefore rationally attributed to insufficient molecular weight, consistent with polymer solution theory where chain length governs entanglement density and load transfer[25,28,41]. Reduced chain length diminishes entanglement density, suppresses viscosity[25], and limits the ability of flow to induce alignment and crystallisation[56]. Consequently, much of the literature focused on developing gentler degumming protocols[25,33,39,57], and alternative solvent systems aimed at preserving or enriching higher MW fibroin

BOX 2 | what does it mean to have a 'good' fibre?

Before discussing the various technologies, it is worth discussing what is a 'good' fibre. From a mechanical perspective, this cannot be reduced to a single parameter. Fibre performance is inherently multidimensional, encompassing strength, Young's modulus, extensibility and toughness modulus. Among these, toughness modulus is often emphasised because it integrates both strength and extensibility as the total area under the stress–strain curve.

Silk, in particular, is frequently celebrated as one of the toughest natural fibres[12,32,119–121], and this reputation and unique selling point has strongly shaped research priorities. As a result, many artificial silk studies focus primarily on maximising toughness as the benchmark of success[41,56,61,93,94,122]. However, identical toughness values can arise from fundamentally different mechanical profiles (Box Fig. 1). A fibre may achieve high toughness modulus through high strength and low extensibility, resisting large loads before fracture. Alternatively, comparable toughness can result from lower strength but very high extensibility. Although the numerical toughness may be the same, the functional behaviour under load differs substantially.

Importantly, native silks are not mechanically uniform materials. Their properties adapt to biological function: dragline silk prioritises strength, while other silks favour extensibility, or adhesion[123]. Furthermore, an individual silk's mechanical performance is tuned through the spinning behaviour itself. Thus, natural silk distinguishes itself not merely by high toughness modulus, but by achieving the appropriate balance of strength and extensibility for its intended role within the structure being spun.

Evaluating whether an artificial fibre is 'good' therefore requires consideration of the full stress–strain response and the intended application, rather than reliance on toughness alone. While this perspective may compare individual metrics at specific points for clarity, readers are encouraged to interpret these values within their broader mechanical and functional context.

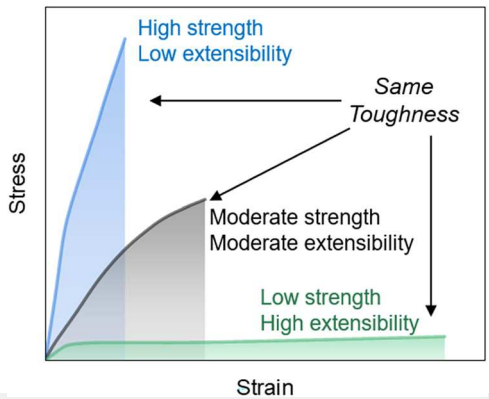

Box Fig 1. Different mechanical pathways to fibre toughness. Stress–strain curves illustrate that fibres can exhibit comparable toughness while differing substantially in tensile strength and extensibility. One profile achieves high toughness through high strength and moderate strain, whereas the another achieves similar energy absorption through lower strength but greater extensibility.

fractions[39,41]. Although direct systematic evaluation of MW on wet-spun RSF fibre mechanical properties has yet to be done, work on RSF films and sponges have shown that a decrease in MW reduces the toughness modulus and strength of the material (Fig. 2A and Box 3)[46,50,58]. These efforts yielded incremental improvements in spinnability and mechanical performance[25,41], reinforcing the view that MW was a dominant bottleneck limiting artificial silk performance. However, high MW alone does not guarantee high mechanical performance. Even sufficiently long chains cannot realise their intrinsic mechanical properties without adequate molecular alignment and packing during spinning[59], highlighting a second main bottleneck.

Across studies that wet-spin aqueous RSF dopes into salt or alcohol-water coagulants, fibre performance consistently increases with MW and the extent of post-spin drawing (Fig. 2A, B). Early aqueous RSF fibres typically exhibit toughness modulus values below 40 MJ m^{-3}[26,60], corresponding to less than ~50% of the toughness modulus of native *B. mori* cocoon brins (90 MJ m^{-3})[32,41]. Improvements in regeneration protocols that retain higher MW fractions (>240 kDa) lead to substantial gains, and when combined with aggressive post-spin drawing, aqueous wet-spun RSF fibres (100–299 MJ m^{-3}) can even exceed the toughness modulus of some native silkworm (*B. mori*, 90 MJ m^{-3}) and certain spider silks (e.g. *Trichonephila pilipes*, 149 MJ m^{-3}) silks[25,32,56,61–65].

Post-drawing is central to these improvements (Fig. 2B)[25]. Tensile drawing aligns chains along the fibre axis, promotes β-sheet formation, reduces defects, enhances load transfer, and decreases fibre diameter, thereby increasing the apparent mechanical propertes[66–68]. In practice, mechanical alignment often exerts a stronger influence on strength and toughness than coagulation chemistry alone[69], indicating that externally imposed deformation can partially compensate for the absence of native spinning gradients. However, this compensation remains limited, as drawing in artificial spinning is fundamentally distinct from spinning in vivo[13,70]. Native silk formation proceeds through a highly evolved pathway, in which the duct, press-like structures, and spinneret impose a specialised and tightly regulated stress environment that cannot be replicated in artificial systems, regardless of whether drawing is applied during spinning or as a post-drawing step. For example, silkworms generate coupled shear and elongational flows within a confined duct, alongside pH gradients and ion exchange, before subsequent restriction via the silk press and spinneret, which generates a complex and continuous stress and solidity gradient during fibre formation[4,13]. This is fundamentally different from wet-spinning in a liquid coagulation bath, where solidification and deformation are decoupled. Although more biomimetic approaches, such as microfluidic spinning[71,72], have been developed, they remain far removed from the complexity of the natural apparatus; consequently, through a combination of our collective knowledge of the 'blueprints' and technical manufacturing capability, no true analogue of the native spinning pathway exists.

Beyond simple chain entanglement, native silk is believed to achieve its impressive mechanical properties because of its complex nanostructural hierarchy[15]. However, only with the addition of additives, such as ions (phosphate) or molecular crowders (dextran/PEO), can degraded aqueous RSF fibres reproduce the hierarchical organisation similar to native silk

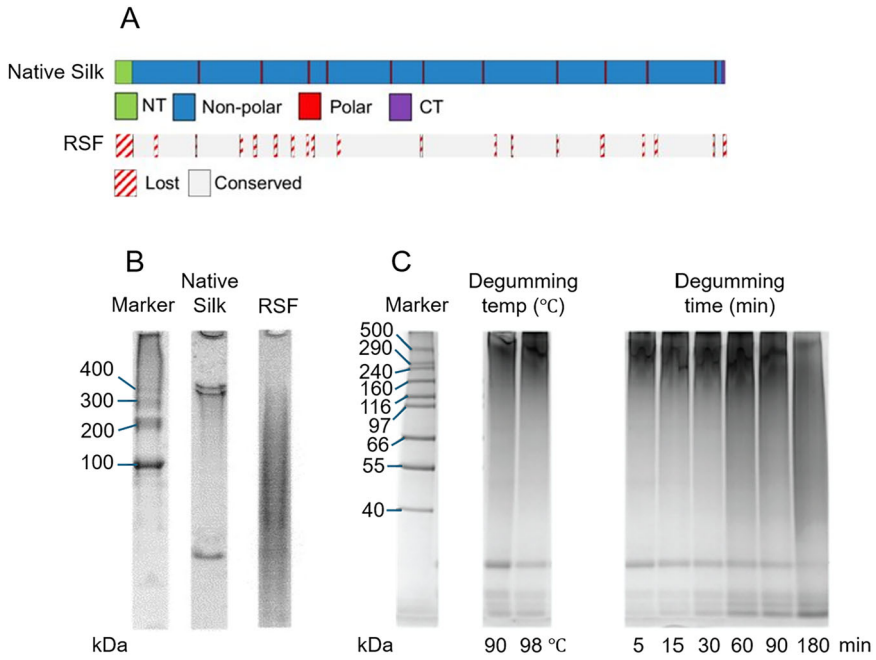

Fig. 1 | The effect of degumming on silk molecular structure. A Schematic illustration of the primary structure of the fibroin heavy chain in native silk and RSF, based on proteomic analysis of the dialysis supernatant, highlighting the loss of the N-terminal with degumming[33]. **B** Sodium dodecyl sulphate-polyacrylamide gel electrophoresis (SDS-PAGE) illustrating the reduction in MW of silk after degumming (see Fig. S1 for unedited PAGE)[40]. **C** SDS-PAGE illustrating the effect of degumming temperature and time on MW (see Fig. S2 for unedited PAGEs)[25]. Adapted with permission[25,33,40]. Copyright © American Chemical Society, Springer Nature and Elsevier Ltd.

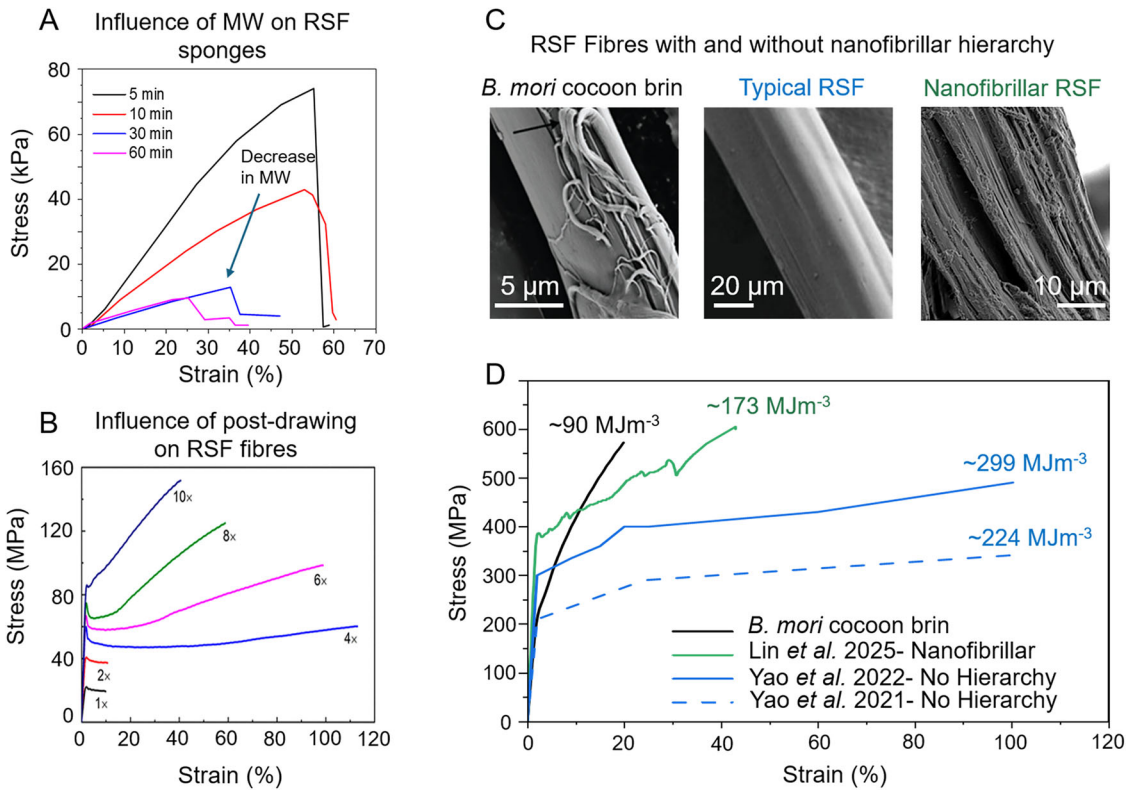

Fig. 2 | Key characteristics of RSF fibres. Owing to the limited availability of data directly correlating MW with fibre mechanical properties, **A** mechanical properties of RSF sponges produced using different degumming times are compared[46]. **B** Effect of post-drawing on the mechanical performance of RSF fibres[25]. **C** SEM images comparing exfoliated native silk cocoon fibres and RSF fibres, highlighting the presence or absence of nanofibrillar hierarchy[25,50,61], and **D** their corresponding representative mechanical properties[56,61,62]. Yao et al.[56] was tested at 0.02 mm/s, Yao et al.[62] at 0.2 mm/s, and the strain rate was not reported for Lin et al.[61]. Adapted with permission[25,46,50,61]. Copyright © American Chemical Society, Elsevier Ltd., Sage Publications.

(Fig. 2C)[61,73]. However, RSFs that better preserve molecular integrity have been reported to generate a nanofibrillar hierarchy without such additives[74]. This indicates that retention of intact terminal domains plays a critical role in enabling biomimetic assembly, allowing hierarchical organisation to emerge intrinsically when key molecular features are preserved. At the same time, the ability of salts or molecular crowders to induce similar structures in more degraded systems indicates that environmental triggers can, at least partially, compensate for lost molecular functionality. As hierarchical

BOX 3 | measuring molecular weight in a multicomponent system

A practical limitation encountered throughout this perspective has been the difficulty of directly comparing MW-property relationships across RSF fibre studies. Many reports do not report MW analysis after degumming or dissolution, or instead rely on qualitative descriptors such as 'native-like or biomimetic' without providing validation, such as a SDS-PAGE or size exclusion chromatography (SEC)[61,122,124–126], despite the well-established sensitivity of RSF properties to degradation during degumming[25,50,55]. As a result, correlations between MW and RSF fibre mechanical properties are frequently inferred rather than directly established, and the only direct comparison could be identified for films or sponges[46,50,58].

More fundamentally, defining 'MW' in silk is non-trivial. RSF often represents a heterogeneous, partially degraded, multi-protein system rather than a single monodisperse polymer. Although SEC and SDS-PAGE are powerful tools for resolving single polymers, species of similar MW often overlap in elution or migration, making it difficult to distinguish intact fibroin chains from partially degraded fragments or associated assemblies. Likewise, dynamic light scattering can provide hydrodynamic size information but assumes spherical particles and does not resolve copolymer interactions or compositional complexity. In practice, SDS-PAGE remains one of the most accessible and robust methods for assessing silk degradation state, particularly when complemented by staining[127,128], or downstream LC-MS or SEC analysis of excised bands[129–131]. While imperfect, these approaches provide a pragmatic means of tracking molecular integrity within an inherently compositionally complex system, such as silk.

Best practice: future studies would benefit from routine reporting of MW distributions with at least SEC or SDS-PAGE, ideally as smear ranges alongside averages, together with complementary analytical methods, enabling more rigorous and reproducible structure-property comparisons across regenerated silk systems.

structuring is hypothesised to enhance toughness[15], one would assume that the tough RSF fibres lacking nanofibrillar hierarchy, such as those spun by Yao et al.[25,56,62], likely fall short of their full mechanical potential. However, across the literature, the toughest RSF fibres reported to exhibit nanofibrillar hierarchy do not outperform the toughest modulus without such features (299 vs. ~173 MJ m^{-3}) (Fig. 2D)[56,61,62].

It is important to note that these comparisons are drawn across independent studies employing different spinning conditions, protein concentrations and testing protocols, and a systematic, side-by-side study isolating hierarchy as a single variable remains absent from the field. Nonetheless, the observation of improved mechanical properties in the absence of well-defined nanofibrillar features demonstrates that hierarchical organisation is not an automatic consequence of mechanical optimisation, and, conversely, that hierarchy is not a strict prerequisite for achieving better mechanical properties. Instead, both hierarchy and mechanical performance are strongly influenced by environmental factors during spinning. Crucially, because many RSF systems do not fully preserve native protein structure, it is challenging to decouple molecular integrity from processing effects. As a result, the influence of spinning environment (ions, hydration, flow and confinement) is often masked by degradation-induced limitations, preventing clear attribution of cause and effect[28]. More importantly, RSF cannot resolve a central question: is hierarchical organisation encoded intrinsically within the native silk protein architecture, does it require external environmental programming to be expressed, or their combination, and if so, to what proportion?

It is worth noting that the ultimate objective of artificial silk spinning research is not simply to respin silk. There is little practical advantage in dissolving an already exceptional natural fibre only to regenerate one that might have similar mechanical properties. The persistence of regeneration approaches therefore suggests a deeper motivation: not merely to reproduce silk, but to understand how silk is made, to identify the physical and chemical principles governing its storage, assembly and solidification, and to translate that understanding into bio-inspired spinning strategies.

Viewed in this light, RSF represents a critical yet fundamentally incomplete step in artificial silk development. It established MW as a prerequisite for spinnability and mechanical performance. However, even as regeneration protocols improved, RSF solutions rarely approached the extreme concentrations[3,26], stability[19] or responsiveness of native silk dopes[28,75,76]. The persistent inability to decouple solubility, stability and alignment foreshadowed a deeper constraint: once molecular integrity is compromised, no amount of downstream processing can fully recover the non-equilibrium assembly pathways used in nature. This realisation set the stage for a second major strategy in artificial silk research, rebuilding the silk molecule from the bottom up.

Recombinant silk proteins: rebuilding the molecule

Recombinant silk proteins emerged as a direct response from the inability to study or use spider silk proteins due to the limitations in farming them, such as their cannibalistic nature[77,78]. However, they can address the molecular limitations of RSF, reframing artificial silk as a problem of molecular design rather than molecular preservation. Instead of attempting to process the inherently difficult-to-solubilise native proteins with harsh chemistries, recombinant approaches sought to reconstruct silk from the bottom up, using genetic engineering to precisely define sequence motifs, terminal domains and repeat architecture[77]. In doing so, recombinant systems can eliminate ambiguity arising from degradation and re-establish MW as a controllable design variable under aqueous processing conditions. At the same time, recombinant systems span a broad design space, with variations that strongly influence assembly pathways, molecular alignment, crystallinity and the resulting performance. Even though a more explicit stratification by construct type would help disentangle limitations arising from molecular design from those imposed by processing conditions, as discussed in detail elsewhere[79–81], this discussion treats recombinant silks in a collective sense, to enable meaningful comparison.

In principle, recombinant systems offer unparalleled molecular precision. Protein sequence, block architecture and terminal domains can be systematically designed, and post-translational modifications can be partially controlled depending on the expression host or co-expressing modifying enzymes, such as kinases[82–84]. This flexibility enables access to silk proteins from species, such as spiders or bagworms[85–87], which are difficult to obtain naturally and, in some cases, exhibit greater toughness modulus than domesticated *B. mori* silk[32]. However, these advantages are counterbalanced by fundamental biological and physiochemical constraints. Expression yields decrease sharply with increasing protein length, as large, repetitive silk-like sequences impose substantial metabolic and proteostasis burdens on host organisms[88–90]. Efforts to increase MW frequently result in intracellular aggregation in the host organism, inclusion body formation, or precipitation during aqueous solution processing and purification[88–90]. Consequently, most recombinant proteins remain significantly shorter than native spider or silkworm silks[89].

As with RSF, inferior recombinant fibre properties were therefore rationally attributed to insufficient MW and chain length[17,91,92]. Consequently, much of the recombinant silk literature focused on engineering longer constructs, through multimerization strategies or blending approaches to increase effective MW and improve spinnability (Fig. 3A–D). These approaches led to clear improvements in fibre formation and mechanical performance, reinforcing the view that molecular reconstruction was the primary bottleneck in recombinant silk systems.

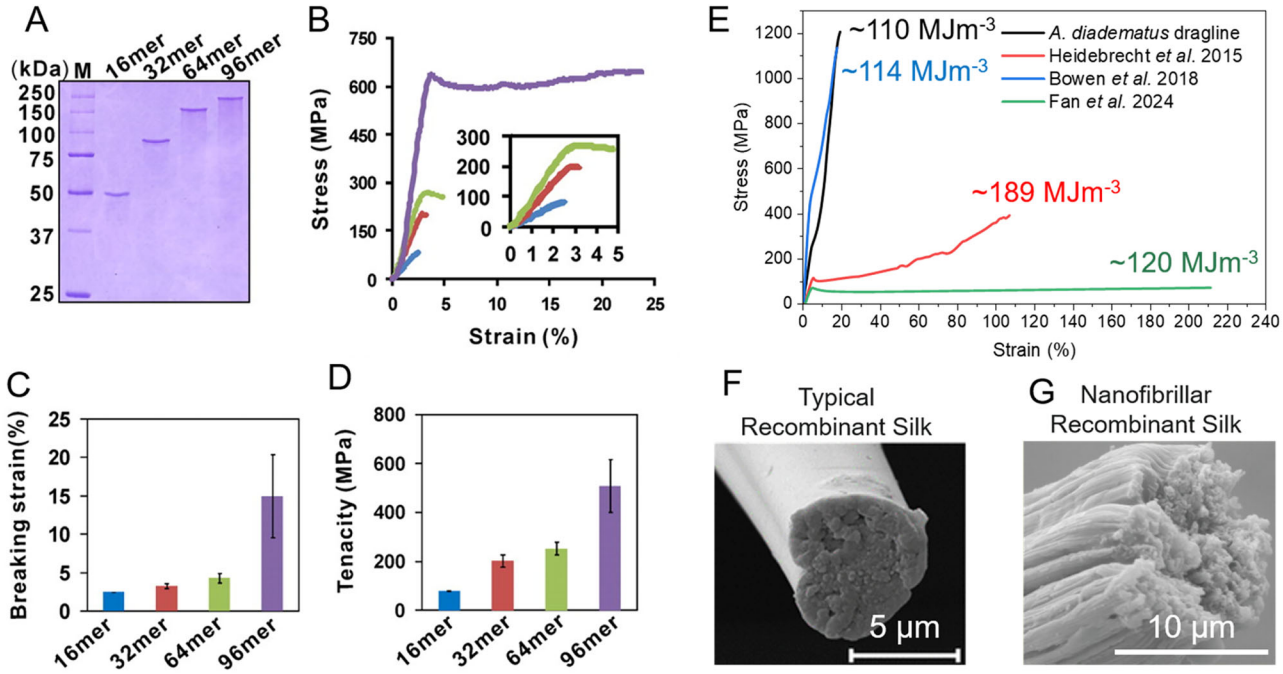

Fig. 3 | Property and structural characteristics of recombinant silk fibres. Influence of MW on recombinant silk fibre performance showing **A** SDS-PAGE analysis demonstrating increase in MW with multimerization, and **B** representative stress–strain curves of the 6-mer (blue), 32-mer (red), 64-mer (green) and 96-mer (purple) fibres, alongside their corresponding **C** extensibility-at-break and **D** strength, where $n = 10$, error bars = SD[17]. **E** Representative stress–strain curves of the toughest reported recombinant silks[91,93,94]. Heidebrecht et al. reported in true stress/true strain, which overestimates material strength[31,93]. SEM images of recombinant silks **F** lacking and **G** exhibiting nanofibrillar hierarchy[91,112]. SEM images should be taken with caution (see Box 4). Adapted with permission[17,91,93,94,112]. Copyright © National Academy of Sciences, American Chemical Society and Wiley.

However, these advances were not without trade-offs. Alongside the biological burdens mentioned above, they often require complex purification requirements in an effort to maximise yield[90]. As a result, past processing routes relied on concentrated salts, denaturants, or non-trivial downstream purification steps that complicate scalability and diminish the environmental advantages often associated with silk[17]. Thus, while recombinant strategies restore molecular control, they do so at the expense of practicality and scalability, introducing significant technical and sustainability constraints.

Under favourable conditions, recombinant silk fibres can achieve high extensibility and toughness, particularly when aggressive post-spin drawing is applied, with reported toughness modulus (114–189 MJ m^{-3}), exceeding some types of native spider silks (*Trichonephila Clavipes*, 111 MJ m^{-3}) (Fig. 3E)[91,93]. This demonstrates that recombinant systems are capable of matching the mechanical performance of natural silk, just like RSF. While RSF fibres typically achieve high toughness modulus through a balance of moderate strength and moderate extensibility, the range of recombinant silk proteins allows for a range of high fibre toughness by shifting the balance between these parameters, increasing strength at the expense of extensibility or vice versa.

Despite these mechanical successes, the interpretation of hierarchical organisation in recombinant silk fibres remains ambiguous (Fig. 3F, G and Box 4). Although nanofibrillar hierarchy is frequently reported, many recombinant spinning protocols employ metal salt buffers such as phosphate[21,42,94–97], conditions known to strongly influence silk protein interactions and self-assembly[19,98]. The frequent use of buffers complicates the interpretation of hierarchical features, as it remains unclear whether the observed ordering arises from intrinsic properties of the recombinant protein architecture or from environmentally driven effects introduced during processing. As in RSF systems, this coupling of molecular design and environmental modulation makes it difficult to disentangle whether hierarchy is encoded within the protein sequence itself or emerges in response to specific ionic conditions. A systematic evaluation that independently controls molecular architecture and environmental variables is therefore required to resolve their relative contributions.

Beyond MW, recombinant systems necessarily simplify the native silk molecular ensemble. Natural silk is a heterogeneous assembly of many proteins that act cooperatively during storage and spinning; however, reconstructing this full compositional complexity via recombinant processing is currently impractical. For example, *B. mori* silk contains over 1000 distinct proteins, although most are present at abundances below 1%[99–101], and major ampullate spider silks contain more than 2000 proteins, 18 of which in quantities above the 1%[102]. Additionally, these proteins are not homogeneously distributed: for example, many of the *B. mori* minor components are localised within the sericin layers rather than the fibroin core[101,102], and the fibroin-sericin ratio correlates with extensional behaviour of the silk dope[103]. Composition, therefore, matters not only in identity but in localisation. The omission of these minor components raises the possibility that recombinant fibres do not fully capture the cooperative molecular interactions that contribute to native assembly, hierarchy or function.

Taken together, recombinant silks represent a second critical but incomplete step in artificial silk development. They demonstrate that improved mechanical properties can be achieved without native molecules, but, like RSF, also show that mechanical properties alone are not diagnostic of native-like assembly. By exposing both the biological limits of producing very large silk proteins and the sensitivity of hierarchical assembly to environmental conditions, recombinant systems demonstrate that molecular design alone is insufficient to reproduce the native spinning pathway. Importantly, most recombinant constructs do not replicate the full architectural complexity of native silks. These insights redirect the field toward a third paradigm: preserving native molecular integrity while systematically reconstructing the physiochemical environment that governs silk assembly in vivo.

BOX 4 | methodological fragility of identifying nanofibrillar hierarchy

Interpretation of wet-spun fibre morphology is further complicated by experimental limitations. Artificially spun fibres may possess 'skins' arising from coagulation speed, which can have very different morphology from the underlying structures[132]. Therefore, surface features resembling nanofibrils can be observed, but this does not necessarily demonstrate that such structures are present throughout the fibre core. Imaging fibre cross-sections can, in principle, address this limitation; however, fracture-based sample preparation introduces additional uncertainty. The manner in which fibres are fractured can generate fibril-like features that reflect crack propagation pathways rather than intrinsic nanofibrillar organisation. Apparent hierarchy may therefore arise from mechanical failure modes rather than native structural architecture. Even within nominally identical fibre batches, nanofibrillar features can vary locally, underscoring the influence of processing history, fracture method and sampling location.

Characterization methods also play a role. SEM, commonly used to visualise nanofibrillar morphology, is highly sensitive to sample preparation. Dehydration, conductive coating and vacuum exposure can introduce morphological artefacts[133]. Atomic force microscopy (AFM) provides a complementary approach, enabling surface topography to be probed under less invasive conditions. However, AFM is also subject to limitations: tip convolution effects can overestimate fibril width and underestimate height[14,134], and the technique is inherently low-throughput, limiting the number of specimens and areas that can be sampled. Consequently, the absence or presence of nanofibrillar features in traditional SEM or AFM images alone cannot be taken as definitive evidence of hierarchical organisation.

While advanced techniques such as focussed ion beam scanning electron microscopy (FIB-SEM) can provide precise imaging of internal structures[135,136], their interpretation still requires caution. For instance, FIB-SEM can introduce artefacts, including curtaining, stripes or streaks arising from variations in milling rates as the ion beam interacts with surface topography, material inhomogeneities or defects[137]. These features may be mistakenly interpreted as nanofibrillar structures[135]. Although such artefacts can be mitigated, for example by milling at an angle, they cannot be entirely excluded[138].

Alternatively, X-ray ptychotomography offers high-resolution imaging without the need for sample preparation that may introduce artefacts[135,139]. However, as a relatively recent and facility-limited technique, its application to native silk remains sparse. Consequently, direct comparison with native silk fibres remains essential for reliable structural interpretation.

Best practice: definitive assessment of hierarchy requires substantial exposure of the fibre interior rather than reliance on surface or partially fractured cross-sections. Ideally, SEM and AFM should be employed in combination to provide complementary structural information across length scales. More rigorous approaches may also include FIB-SEM, X-ray ptychotomography and controlled mechanical or ultrasonic dispersion of fibres, performed alongside microscopy[140], to determine whether discrete nanofibrillar substructures can be reproducibly isolated and quantitatively assessed. Additionally, images acquired at multiple length scales and from multiple locations should be reported to demonstrate that the observed morphology is representative. Until such multimodal validation becomes routine, caution is warranted when correlating SEM- or AFM-derived morphology as definitive evidence of molecular hierarchy.

Preserving molecular weight and composition

Numerous studies have reported methods that minimise fibroin degradation during degumming, including enzymatic degumming, microwave-assisted extraction, or the production of silk cocoons with reduced β-sheets that can be degummed under gentler conditions[39,51,104]. However, while maintaining fibroin's molecular weight, these approaches still differ fundamentally from the native silk gland because they do not retain sericin or the other trace proteins found in spun cocoons. To address this, recent work has focussed on developing methods to regenerate silk solution that avoid degumming altogether to produce a 'RUS' that preserves the native multicomponent molecular architecture prior to processing (Fig. 4)[19,40,41,105]. RUS eliminates the need for degumming by solubilising the entire silk material. As a result, it produces distinct, well-defined bands on SDS-PAGE, in contrast to the smeared profiles typically seen with conventional alkaline degummed RSF. Beyond the improved molecular weight preservation achieved with gentler degumming methods, RUS yields solutions containing intact, multicomponent protein assemblies, enabling direct investigation of less degraded silk dopes that more closely resemble the complex in nature. Nevertheless, it remains possible that some degree of degradation is present. Notably, dissolution of undegummed silk, most commonly using lithium bromide, has long been employed to extract and characterise silk proteins for proteomic analysis[106,107]. In this context, several silk-producing species have been dissolved without prior degumming, including silverfish, pantry moth and cricket silks (Figs. 4A–D and S3–S6)[105–109]. Despite this precedent, relatively few studies have explored functional applications, and to date, only one report has spun fibres using RUS solutions[41,105,109].

A distinguishing feature of *B. mori* RUS is that it inherently undergoes LLPS under aqueous conditions as a function of concentration (Fig. 4E)[41]. This behaviour likely arises from the retention of sericin and other native silk proteins, including P25 and lower-abundance components, and their interactions with the fibroin complex. Together, these proteins form multicomponent assemblies that more closely resemble the native silk molecular ensemble, rather than simplified single protein solutions[22,110]. In addition to promoting LLPS, retained sericin likely contributes to the enhanced solution stability of RUS dopes by modulating hydration, screening intermolecular attractions and reducing the propensity for premature aggregation[41,111]. The emergence of LLPS and improved metastability without external additives mirrors behaviour increasingly recognised in native silk dopes and highlights the importance of multicomponent protein systems for achieving biomimetic solution states[21,22,110].

Within this framework, RUS addresses the MW and structural integrity constraints that defined both RSF and recombinant silk systems. Fibres spun from aqueous RUS dopes exhibit hierarchical features that approach those of native cocoon silk, including nanofibrillar organisation and multiscale ordering (Fig. 4F)[41]. Importantly, this recovery of hierarchy occurs without genetic reconstruction, extensive molecular engineering, or the addition of metal ions, suggesting that preservation of native molecular architecture and compositional complexity is sufficient to unlock biologically relevant assembly pathways under aqueous processing conditions.

Earlier attempts to induce hierarchical organisation in RSF or Recombinant systems have demonstrated that environmental modulation alone may promote aspects of nanofibrillar assembly. In particular, the addition of salts or molecular crowders to RSF or Recombinant dopes has been reported to trigger LLPS formation and concurrently nanofibrillar structures under aqueous conditions[41,42,61,112,113]. However, although individual variables can be systematically screened in isolation, these strategies inherently modify solution composition, intermolecular interactions and processing conditions simultaneously. As a result, once the full system is reconstituted, it becomes difficult to disentangle the respective contributions of MW, compositional complexity and environmental cues to the

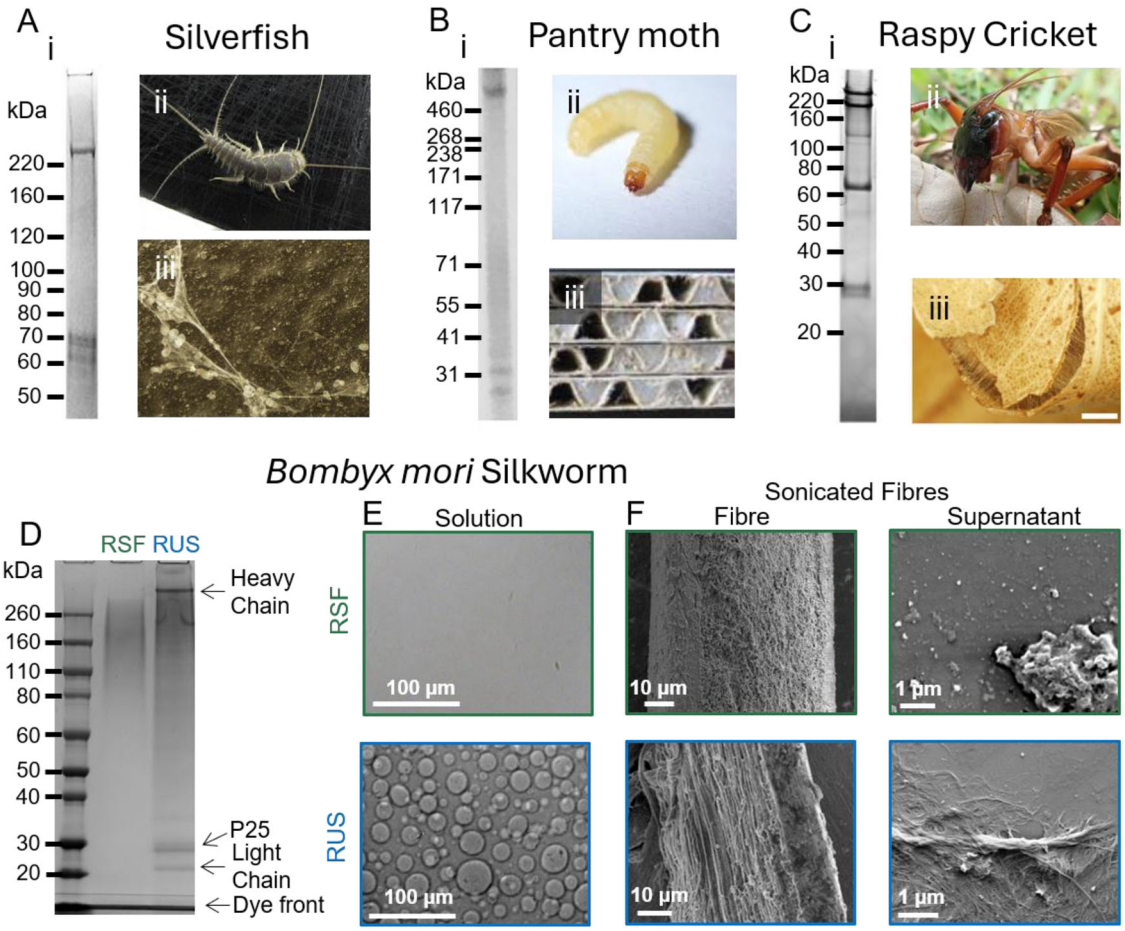

Fig. 4 | Preservation of molecular integrity and hierarchical features in RUS. Representative SDS-PAGE profiles of RUS obtained from a range of ii silk-producing organisms and iii their silk structures, including **A** silverfish (*Lepisma saccharina*)[108], **B** pantry moth (*Plodia interpunctella*)[105,118] and **C** raspy cricket (Gryllacrididae, photo credit: Peter T. Ruhr), (see Figs. S3–S5 for unedited PAGEs)[106]. **E** Comparative SDS-PAGE of RSF and RUS dopes, highlighting differences in molecular weight distribution and preservation of intact protein structure in RUS (see Fig. S6 for unedited PAGE)[41]. **F** Microscopy images demonstrating intrinsic LLPS in RUS, absent in RSF[41]. **D** Sonicated wet-spun fibres revealing nanofibrillar organisation in RUS that is not observed in RSF[41]. Adapted with permission[41,105,106,108,118]. Copyright © Elsevier Ltd., American Chemical Society, Wiley and PLOS.

emergence of hierarchical organisation. In this context, RUS provides a complementary platform in which intact molecular architecture and multicomponent composition are preserved, allowing environmental factors to be examined without the confounding effects of molecular degradation[19].

Despite these advances, RUS is not equivalent to native silk (Fig. 5). Although it preserves molecular weight and multicomponent protein composition, its rheological behaviour differs markedly from that of native silk gland dopes (Fig. 5A, B)[41,114,115]. At comparable protein concentrations, native silk is several orders of magnitude stiffer and more viscous, exhibiting highly tuned viscoelastic and shear-responsive behaviour. Given that RUS retains high molecular fidelity, this rheological disparity cannot be attributed solely to differences in primary structure or MW. Notably, RUS also contains sericin, whereas the posterior section of the middle gland, typically analysed, does not. Native sericin obtained from mutagenic silkworms without fibroin was found to have a lower viscosity than those with fibroin[116]. Therefore, sericin might partially account for some of the observed differences. However, the influence of sericin on the rheology of multicomponent silk solutions in vitro remains unclear, largely due to the lack of methods for extracting undegraded sericin. Until such approaches are developed, the independent rheological contributions of intact sericin and fibroin cannot be reliably assessed. Moreover, the physiochemical environment of regenerated systems differs from that of native silk. For instance, altering the pH of RSF led to significant differences in their frequency sweep profiles[33], with moduli more similar to native silk, indicating the importance of pH in mimicking the rheology. Collectively, these observations point to the critical role of the native gland environment.

RUS solutions are generated under homogeneous bulk dissolution conditions and therefore lack this non-equilibrium physiological regulation. Although post-spin drawing and ethanol annealing serve as critical secondary processing steps that can promote β-sheet formation, enhance crystallinity and improve molecular alignment beyond that achieved during primary fibre formation alone, aqueous wet-spun RUS fibres, despite exhibiting toughness modulus and extensibility that can exceed native values, do not yet reproduce the degree of molecular alignment observed in native cocoon silk (Fig. 5C–G)[41]. These remaining discrepancies are informative: it indicates that although intact molecular structure and multicomponent solution behaviour is sufficient to recover hierarchical assembly and high mechanical performance, it is not sufficient to recreate native rheology or alignment. Molecular fidelity enables the possibility of biomimetic assembly; it does not guarantee its execution.

Viewed in this context, RUS helps to clarify some of the molecular challenges inherent to artificial silk research. By preserving the molecular weight distribution and associated components, it enables a clearer separation between molecular fidelity and downstream processing (spinning) effects than is typically possible in conventional regenerated systems. While this still represents only an approximation of the native gland contents, it allows certain molecular uncertainties to be reduced and provides a useful point of comparison across artificial silk platforms. Rather than

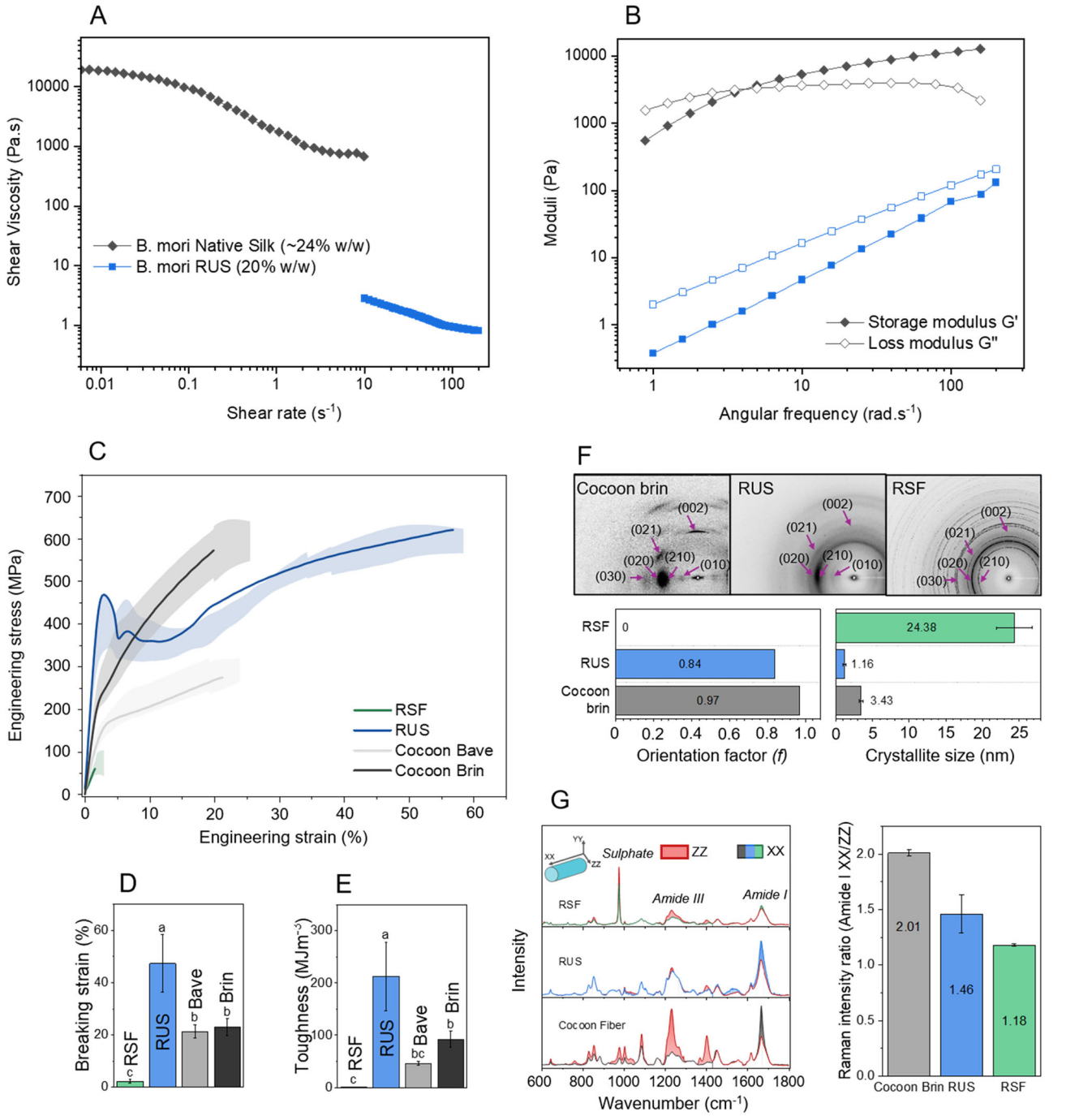

Fig. 5 | Comparison of RUS and native *B. mori* silk. Rheological comparison of dopes by **A** shear sweep and **B** frequency sweep, demonstrating that native silk exhibits viscoelastic properties and substantially higher viscosity and moduli than RUS at comparable concentrations (RUS frequency sweep is unpublished data, M. Zaki, B. Allardyce, 2025)[41,114,115]. **C** Representative stress–strain curves with shaded regions indicating standard deviation, showing that RUS fibres exhibit greater **D** extensibility and **E** toughness than native silk under the conditions tested, where $n = 5$, error bars = SD. However, alignment measured with **F** wide-angle X-ray scattering (WAXS) and **G** polarised Raman demonstrates that RUS fibres possess a lower degree of molecular alignment compared to native *B. mori* silk, where $n = 3$, error bars = SD. Adapted with permission[41,114]. Copyright © Wiley, American Chemical Society and MDPI.

resolving the system, RUS helps frame the remaining challenges, which increasingly appear to lie not only in molecular composition but also in the physicochemical conditions of the silk gland, including controlled ionic gradients, dehydration dynamics and elongational flow that couple molecular interactions to fibre scale alignment.

In this sense, RUS provides a useful diagnostic platform for exploring the constraints governing biomimetic silk assembly. It shifts the focus of artificial silk research from solely molecular optimisation toward a broader consideration of the environmental conditions that regulate silk formation. By demonstrating that multicomponent silk proteins can undergo LLPS and hierarchical assembly under aqueous conditions when molecular integrity is reasonably preserved, RUS offers a framework for systematically exploring how environmental cues regulate alignment and final fibre performance. Together, these observations reinforce the view that effective biomimicry likely requires not only molecular fidelity, but also appropriate compositional and environmental context.

Outlook

For much of its history, artificial silk research has framed performance gaps as molecular deficiencies. RSF revealed the consequences of degradation, and recombinant systems sought to rebuild sequence and architecture with precision. More recent systems, including RUS, indicate that when molecular integrity is better preserved, several previously assumed 'molecular limits' become less restrictive. Notably, fibres produced from all three platforms can, under certain conditions, achieve mechanical properties that equal or even surpass those of native silk. Together, these observations suggest that the principal bottleneck may no longer reside solely in MW or sequence design.

Importantly, hierarchical organisation and LLPS are not unique to one system. In both RSF and recombinant systems, the addition of salts or molecular crowders can induce LLPS and promote nanofibrillar assembly under aqueous conditions. These observations demonstrate that environmental modulation alone can drive aspects of hierarchy, even when molecular integrity is imperfect. However, because such additives simultaneously alter ionic strength, hydration and intermolecular interactions, it can be difficult to disentangle intrinsic molecular effects from externally imposed environmental stress.

In contrast, RUS exhibits LLPS intrinsically as a function of concentration, without requiring salts or exogenous molecular crowders. This behaviour suggests that retained, less abundant cocoon proteins may contribute to multicomponent interactions as molecular crowders that promote phase separation and nanofibrillar formation. Rather than introducing hierarchy through external additives, RUS appears to enable it through preserved compositional complexity. Even so, its rheology remains substantially different from native gland silk[3,41,117], and molecular alignment in spun fibres does not yet fully match that achieved in vivo[41].

Taken together, these comparisons reinforce a broader conclusion: mechanical properties, hierarchy and LLPS can be achieved through multiple routes, but reproducing the tightly regulated, non-equilibrium physiochemical and rheological environment of the silk gland remains unresolved. The next phase of artificial silk research will likely focus less on further molecular optimisation and more on reconstructing multicomponent systems within controlled ionic, hydration and flow landscapes that couple phase behaviour to structure development.

Data availability

All data supporting the findings of this study are available within the paper and its Supplementary Information.

Received: 27 March 2026; Accepted: 4 June 2026;
Published online: 25 June 2026

References

1. Blamires, S. *Silk: Exploring Nature's Superfibre* (Xlibris, 2022).
2. Holland, C., Vollrath, F., Ryan, A. J. & Mykhaylyk, O. O. Silk and synthetic polymers: reconciling 100 degrees of separation. *Adv. Mater.* **24**, 105–109 (2012).
3. Laity, P. R., Gilks, S. E. & Holland, C. Rheological behaviour of native silk feedstocks. *Polymer* **67**, 28–39 (2015).
4. Andersson, M., Johansson, J. & Rising, A. Silk spinning in silkworms and spiders. *Int J. Mol. Sci.* **17**, 1290 (2016).
5. Andersson, M. et al. Carbonic anhydrase generates CO_2 and H^+ that drive spider silk formation via opposite effects on the terminal domains. *PLOS Biol.* **12**, e1001921 (2014).
6. Domigan, L. J. et al. Carbonic anhydrase generates a pH gradient in *Bombyx mori* silk glands. *Insect Biochem. Mol. Biol.* **65**, 100–106 (2015).
7. Zhou, L., Chen, X., Shao, Z., Huang, Y. & Knight, D. P. Effect of metallic ions on silk formation in the mulberry silkworm, *Bombyx mori*. *J. Phys. Chem. B* **109**, 16937–16945 (2005).
8. Zhou, L. et al. Copper in the silk formation process of *Bombyx mori* silkworm. *FEBS Lett.* **554**, 337–341 (2003).
9. Liu, Q. et al. Dynamic changes and characterization of the metal ions in the silk glands and silk fibers of silkworm. *Int. J. Mol. Sci.* **24**, 6556 (2023).
10. Brookstein, O. et al. Metal ions guide the production of silkworm silk fibers. *Nat. Commun.* **15**, 6671 (2024).
11. Song, K. et al. Decoding silkworm spinning programmed by pH and metal ions. *Sci. Bull.***69**, 792–802 (2024).
12. Vollrath, F. & Knight, D. P. Liquid crystalline spinning of spider silk. *Nature* **410**, 541–548 (2001).
13. Sparkes, J. & Holland, C. Analysis of the pressure requirements for silk spinning reveals a pultrusion dominated process. *Nat. Commun.* **8**, 594 (2017).
14. Greving, I., Cai, M., Vollrath, F. & Schniepp, H. C. Shear-induced self-assembly of native silk proteins into fibrils studied by atomic force microscopy. *Biomacromolecules* **13**, 676–682 (2012).
15. Qiu, W., Patil, A., Hu, F. & Liu, X. Y. Hierarchical structure of silk materials versus mechanical performance and mesoscopic engineering principles. *Small* **15**, 1903948 (2019).
16. Ling, S., Kaplan, D. L. & Buehler, M. J. Nanofibrils in nature and materials engineering. *Nat. Rev. Mater.* **3**, 18016 (2018).
17. Xia, X.-X. et al. Native-sized recombinant spider silk protein produced in metabolically engineered *Escherichia coli* results in a strong fiber. *Proc. Natl. Acad. Sci. USA*. **107**, 14059–14063 (2010).
18. Li, Q., Jiang, Y. & Chen, Y. The regulatory principles, physiological functions, and phase transition of biomolecular condensates. *Front. Cell Dev. Biol.* **14**, 1759561 (2026).
19. Zaki, M. et al. Anions, not cations, drive silk stability and self-assembly: insights from regenerated undegummed silk. *ACS Biomater. Sci. Eng.* **11**, 5285–5292 (2025).
20. Zaki, M. et al. Phosphate ions reverse the phase composition of silk fibroin condensates. *Mater. Horiz.* https://doi.org/10.1039/D6MH00013D (2026).
21. Lay, M. G., Oktaviani, N. A., Malay, A. D. & Numata, K. Exploring the self-assembly of silk proteins through liquid-liquid phase separation. *Polym. J.* **57**, 799–814 (2025).
22. Eliaz, D. et al. Micro and nano-scale compartments guide the structural transition of silk protein monomers into silk fibers. *Nat. Commun.* **13**, 7856 (2022).
23. Vollrath, F. The complexity of silk under the spotlight of synthetic biology. *Biochem. Soc. Trans.* **44**, 1151–1157 (2016).
24. Miyake, S. & Azuma, M. Acidification of the silk gland lumen in *Bombyx mori* and *Samia cynthia ricini* and localization of H^+-translocating vacuolar-type ATPase. *J. Insect Biotechnol. Sericology* **77**, 9–16 (2008).
25. Yao, Y. et al. Improving the tensile properties of wet spun silk fibers using rapid Bayesian algorithm. *ACS Biomater. Sci. Eng.* **6**, 3197–3207 (2020).
26. Koeppel, A. & Holland, C. Progress and trends in artificial silk spinning: a systematic review. *ACS Biomater. Sci. Eng.* **3**, 226–237 (2017).
27. Vollrath, F. & Porter, D. Silks as ancient models for modern polymers. *Polymer* **50**, 5623–5632 (2009).
28. Holland, C., Terry, A. E., Porter, D. & Vollrath, F. Natural and unnatural silks. *Polymer* **48**, 3388–3392 (2007).
29. Viney, C., Huber, A. E., Dunaway, D. L., Case, S. T. & Kaplan, D. L. Processing natural and reconstituted silk solutions under equilibrium and non-equilibrium conditions. *MRS Online Proc. Libr.* **292**, 211–217 (1992).
30. Koebley, S. R. et al. Silk reconstitution disrupts fibroin self-assembly. *Biomacromolecules* **16**, 2796–2804 (2015).
31. Greco, G., Schmuck, B., Jalali, S. K., Pugno, N. M. & Rising, A. Influence of experimental methods on the mechanical properties of silk fibers: a systematic literature review and future road map. *Biophys. Rev.* **4**, 031301 (2023).

32. Braxton, T., Holland, C. & Greco, G. The circular argument behind spider and silkworm silk mechanical properties. *Mater. Des.* **260**, 115224 (2025).
33. Moreno-Tortolero, R. O. et al. Molecular organization of fibroin heavy chain and mechanism of fibre formation in *Bombyx mori*. *Commun. Biol.* **7**, 786 (2024).
34. He, Y.-X. et al. N-terminal domain of *Bombyx mori* fibroin mediates the assembly of silk in response to pH decrease. *J. Mol. Biol.* **418**, 197–207 (2012).
35. Gaines, W. A., Sehorn, M. G. & Marcotte, W. R. Jr Spidroin N-terminal domain promotes a pH-dependent association of silk proteins during self-assembly. *J. Biol. Chem.* **285**, 40745–40753 (2010).
36. Schaefer, C. & McLeish, T. C. B. Theoretical rheo-physics of silk: intermolecular associations reduce the critical specific work for flow-induced crystallization. *J. Rheol.* **66**, 515–534 (2022).
37. Schaefer, C., Laity, P. R., Holland, C. & McLeish, T. C. B. Silk protein solution: a natural example of sticky reptation. *Macromolecules* **53**, 2669–2676 (2020).
38. Ferry, J. D. *Viscoelastic Properties of Polymers*, 3rd edn (Wiley, 1980).
39. Wöltje, M., Kölbel, A., Aibibu, D. & Cherif, C. A fast and reliable process to fabricate regenerated silk fibroin solution from degummed silk in 4 hours. *Int. J. Mol. Sci.* **22**, 10565 (2021).
40. Yamada, H., Nakao, H., Takasu, Y. & Tsubouchi, K. Preparation of undegraded native molecular fibroin solution from silkworm cocoons. *Mater. Sci. Eng. C* **14**, 41–46 (2001).
41. Zaki, M. et al. Recreating silk's fibrillar nanostructure by spinning solubilized, undegummed silk. *Adv. Mater.* **37**, 2413786 (2025).
42. Malay, A. D. et al. Spider silk self-assembly via modular liquid-liquid phase separation and nanofibrillation. *Sci. Adv.* **6**, eabb6030 (2020).
43. Koeppel, A., Stehling, N., Rodenburg, C. & Holland, C. Spinning beta silks requires both ph activation and extensional stress. *Adv. Funct. Mater.* **31**, 2103295 (2021).
44. Holland, C., Numata, K., Rnjak-Kovacina, J. & Seib, F. P. The biomedical use of silk: past, present, future. *Adv. Healthc. Mater.* **8**, 1800465 (2019).
45. Allardyce, B. J. et al. Glycerol-plasticised silk membranes made using formic acid are ductile, transparent and degradation-resistant. *Mater. Sci. Eng. C* **80**, 165–173 (2017).
46. Rnjak-Kovacina, J. et al. Lyophilized silk sponges: a versatile biomaterial platform for soft tissue engineering. *ACS Biomater. Sci. Eng.* **1**, 260–270 (2015).
47. Zhu, R. et al. An artificial liquid–liquid phase separation-driven silk fibroin-based adhesive for rapid hemostasis and wound sealing. *Acta Biomater.* **182**, 14–27 (2024).
48. Gheysens, T., Collins, A., Raina, S., Vollrath, F. & Knight, D. P. Demineralization enables reeling of wild silkmoth cocoons. *Biomacromolecules* **12**, 2257–2266 (2011).
49. Chen, F., Porter, D. & Vollrath, F. Morphology and structure of silkworm cocoons. *Mater. Sci. Eng. C* **32**, 772–778 (2012).
50. Allardyce, B. J. et al. The impact of degumming conditions on the properties of silk films for biomedical applications. *Text. Res. J.* **86**, 275–287 (2016).
51. Freddi, G., Mossotti, R. & Innocenti, R. Degumming of silk fabric with several proteases. *J. Biotechnol.* **106**, 101–112 (2003).
52. Haggag, K., El-Sayed, H. & Allam, O. G. Degumming of silk using microwave-assisted treatments. *J. Nat. Fibers* **4**, 1–22 (2007).
53. Kalita, M., Allardyce, B. J., Sankaranarayanan, K., Devi, D. & Rajkhowa, R. Sericin from mulberry and non-mulberry silk using chemical-free degumming. *J. Text. Inst.* **113**, 2080–2089 (2022).
54. Gupta, D., Agrawal, A., Chaudhary, H., Gulrajani, M. & Gupta, C. Cleaner process for extraction of sericin using infrared. *J. Clean. Prod.* **52**, 488–494 (2013).
55. Bucciarelli, A., Greco, G., Corridori, I., Pugno, N. M. & Motta, A. A design of experiment rational optimization of the degumming process and its impact on the silk fibroin properties. *ACS Biomater. Sci. Eng.* **7**, 1374–1393 (2021).
56. Yao, Y. et al. Spinning regenerated silk fibers with improved toughness by plasticizing with low molecular weight silk. *Biomacromolecules* **22**, 788–799 (2021).
57. Rastogi, S. & Kandasubramanian, B. Processing trends of silk fibers: silk degumming, regeneration and physical functionalization. *J. Text. Inst.* **111**, 1794–1810 (2020).
58. Kim, H. J. et al. Effect of degumming methods on structural characteristics and properties of regenerated silk. *Int. J. Biol. Macromol.* **104**, 294–302 (2017).
59. Mortimer, B., Guan, J., Holland, C., Porter, D. & Vollrath, F. Linking naturally and unnaturally spun silks through the forced reeling of *Bombyx mori*. *Acta Biomater.* **11**, 247–255 (2015).
60. Matsumoto, K., Uejima, H., Iwasaki, T., Sano, Y. & Sumino, H. Studies on regenerated protein fibers. III. Production of regenerated silk fibroin fiber by the self-dialyzing wet spinning method. *J. Appl. Polym. Sci.* **60**, 503–511 (1996).
61. Lin, Q. et al. From snapshot to movie: visualizing native silk spinning defines the paradigm for bio-inspired spinning. *Adv. Funct. Mater.* **36**, e11413 (2026).
62. Yao, Y. et al. Toughening wet-spun silk fibers by silk nanofiber templating. *Macromol. Rapid Commun.* **43**, 2100891 (2022).
63. Yan, J., Zhou, G., Knight, D. P., Shao, Z. & Chen, X. Wet-spinning of regenerated silk fiber from aqueous silk fibroin solution: discussion of spinning parameters. *Biomacromolecules* **11**, 1–5 (2010).
64. Zhang, F. et al. Regeneration of high-quality silk fibroin fiber by wet spinning from $CaCl_2$–formic acid solvent. *Acta Biomater.* **12**, 139–145 (2015).
65. Kerr, G. G. et al. Mechanical properties of silk of the Australian golden orb weavers *Nephila pilipes* and *N. plumipes*. *Biol. Open* **7**, bio029249 (2018).
66. Keten, S., Xu, Z., Ihle, B. & Buehler, M. J. Nanoconfinement controls stiffness, strength and mechanical toughness of β-sheet crystals in silk. *Nat. Mater.* **9**, 359–367 (2010).
67. Giesa, T., Arslan, M., Pugno, N. M. & Buehler, M. J. Nanoconfinement of spider silk fibrils begets superior strength, extensibility, and toughness. *Nano Lett.* **11**, 5038–5046 (2011).
68. Porter, D., Guan, J. & Vollrath, F. Spider silk: super material or thin fibre? *Adv. Mater.* **25**, 1275–1279 (2013).
69. Schmuck, B. et al. Impact of physio-chemical spinning conditions on the mechanical properties of biomimetic spider silk fibers. *Commun. Mater.* **3**, 83 (2022).
70. Asakura, T. et al. Some observations on the structure and function of the spinning apparatus in the silkworm *Bombyx mori*. *Biomacromolecules* **8**, 175–181 (2007).
71. Peng, Q., Shao, H., Hu, X. & Zhang, Y. Microfluidic dry-spinning and characterization of regenerated silk fibroin fibers. *J. Vis. Exp.* **127**, 56271 (2017).
72. Chen, J. et al. Replicating shear-mediated self-assembly of spider silk through microfluidics. *Nat. Commun.* **15**, 527 (2024).
73. Yang, S. et al. Calcium ion-triggered liquid-liquid phase separation of silk fibroin and spinning through acidification and shear stress. *Nat. Commun.* **15**, 10394 (2024).
74. Moreno-Tortolero, R. O. et al. Manipulating the water–air interface to drive protein assembly for functional silk-like fibroin fibre production. *Commun. Mater.* **5**, 277 (2024).
75. Schaefer, C., Laity, P. R., Holland, C. & McLeish, T. C. B. Stretching of *Bombyx mori* silk protein in flow. *Molecules* **26**, 1663 (2021).
76. Laity, P. R. & Holland, C. Seeking solvation: exploring the role of protein hydration in silk gelation. *Molecules* **27**, 551 (2022).
77. Schacht, K. & Scheibel, T. Processing of recombinant spider silk proteins into tailor-made materials for biomaterials applications. *Curr. Opin. Biotechnol.* **29**, 62–69 (2014).

78. Wöltje, M. & Böbel, M. Natural biodegradable medical polymers: silk. in (ed. Zhang, X.) *Science and Principles of Biodegradable and Bioresorbable Medical Polymers*, Ch. 12, 351–376 (Woodhead Publishing, 2017).
79. Schmuck, B. et al. Strategies for making high-performance artificial spider silk fibers. *Adv. Funct. Mater.* **34**, 2305040 (2024).
80. Zheng, K. & Ling, S. De novo design of recombinant spider silk proteins for material applications. *Biotechnol. J.* **14**, 1700753 (2019).
81. Sutherland, T. D., Huson, M. G. & Rapson, T. D. Rational design of new materials using recombinant structural proteins: current state and future challenges. *J. Struct. Biol.* **201**, 76–83 (2018).
82. Breslauer, D. N. Current progress on scale-up and commercialization of microbially-produced silk. *Adv. Funct. Mater.* **35**, 2408386 (2025).
83. Rabotyagova, O. S., Cebe, P. & Kaplan, D. L. Protein-based block copolymers. *Biomacromolecules* **12**, 269–289 (2011).
84. Möttönen, N. B. et al. Induced proximity approach enables the recombinant production of polyphosphorylated silk proteins with improved adhesiveness. *Biomacromolecules* **26**, 8594–8605 (2025).
85. Zhao, S. et al. Recombinant silk proteins with additional polyalanine have excellent mechanical properties. *Int. J. Mol. Sci.* **22**, 1513 (2021).
86. Zhang, P. et al. Bagworm silk-mimetic protein fibers with extraordinary stiffness via in vivo polymerization and hierarchical self-assembly. *Adv. Funct. Mater.* **35**, 2416526 (2025).
87. Lu, W. et al. A review on complete silk gene sequencing and de novo assembly of artificial silk. *Int. J. Biol. Macromol.* **264**, 130444 (2024).
88. Hussain, H., Fisher, D. I., Abbott, W. M., Roth, R. G. & Dickson, A. J. Use of a protein engineering strategy to overcome limitations in the production of “difficult to express” recombinant proteins. *Biotechnol. Bioeng.* **114**, 2348–2359 (2017).
89. Dinjaski, N. & Kaplan, D. L. Recombinant protein blends: silk beyond natural design. *Curr. Opin. Biotechnol.* **39**, 1–7 (2016).
90. Schmuck, B., Greco, G., Shilkova, O. & Rising, A. Effects of mini-spidroin repeat region on the mechanical properties of artificial spider silk fibers. *ACS Omega* **9**, 42423–42432 (2024).
91. Bowen, C. H. et al. Recombinant spidroins fully replicate primary mechanical properties of natural spider silk. *Biomacromolecules* **19**, 3853–3860 (2018).
92. Li, X., Shi, C. H., Tang, C. L., Cai, Y. M. & Meng, Q. The correlation between the length of repetitive domain and mechanical properties of the recombinant flagelliform spidroin. *Biol. Open* **6**, 333–339 (2017).
93. Heidebrecht, A. et al. Biomimetic fibers made of recombinant spidroins with the same toughness as natural spider silk. *Adv. Mater.* **27**, 2189–2194 (2015).
94. Fan, R. et al. Sustainable spinning of artificial spider silk fibers with excellent toughness and inherent potential for functionalization. *Adv. Funct. Mater.* **35**, 2410415 (2024).
95. Humenik, M., Smith, A. M., Arndt, S. & Scheibel, T. Ion and seed dependent fibril assembly of a spidroin core domain. *J. Struct. Biol.* **191**, 130–138 (2015).
96. Li, M. et al. Artificial spider silk via edge-cysteine–locked β-sheet assembly. *Adv. Sci.* **13**, e17615 (2026).
97. Qi, X. et al. Spider silk protein forms amyloid-like nanofibrils through a non-nucleation-dependent polymerization mechanism. *Small* **19**, e2304031 (2023).
98. Wigham, C., Varude, V., O’Donnell, H. & Zha, R. H. The role of phosphate in silk fibroin self-assembly: a Hofmeister study. *Soft Matter* **21**, 2461–2470 (2025).
99. Yi, Q. et al. Shotgun proteomic analysis of the *Bombyx mori* anterior silk gland: an insight into the biosynthetic fiber spinning process. *Proteomics* **13**, 2657–2663 (2013).
100. Dong, Z. et al. Comparative proteomics reveal diverse functions and dynamic changes of *Bombyx mori* silk proteins spun from different development stages. *J. Proteome Res.* **12**, 5213–5222 (2013).
101. Zhang, Y. et al. Comparative proteome analysis of multi-layer cocoon of the silkworm, *Bombyx mori*. *PLoS ONE* **10**, e0123403 (2015).
102. Sonavane, S. et al. Origin, structure, and composition of the spider major ampullate silk fiber revealed by genomics, proteomics, and single-cell and spatial transcriptomics. *Sci. Adv.* **10**, eadn0597 (2024).
103. Välisalmi, T. & Linder, M. B. The ratio of fibroin to sericin in the middle silk gland of *Bombyx mori* and its correlation with the extensional behavior of the silk dope. *Protein Sci.* **33**, e4907 (2024).
104. Boulet-Audet, M., Holland, C., Gheysens, T. & Vollrath, F. Dry-spun silk produces native-like fibroin solutions. *Biomacromolecules* **17**, 3198–3204 (2016).
105. Eccles, L. E., Orozco, A. A., Liwang, R. K. & Stoppel, W. L. Self-assembly of plodia interpunctella silk particles: mechanisms and encapsulation strategies. *Ind. Eng. Chem. Res.* **64**, 14913–14926 (2025).
106. Walker, A. A. et al. Silk from crickets: a new twist on spinning. *PLoS ONE* **7**, e30408 (2012).
107. Sezutsu, H. et al. Identification of four major hornet silk genes with a complex of alanine-rich and serine-rich sequences in *Vespa simillima* xanthoptera Cameron. *Biosci. Biotechnol. Biochem.* **71**, 2725–2734 (2007).
108. Walker, A. A., Church, J. S., Woodhead, A. L. & Sutherland, T. D. Silverfish silk is formed by entanglement of randomly coiled protein chains. *Insect Biochem. Mol. Biol.* **43**, 572–579 (2013).
109. Kameda, T. Influence of pH, temperature, and concentration on stabilization of aqueous hornet silk solution and fabrication of salt-free materials. *Biopolymers* **103**, 41–52 (2015).
110. Miali, M. E., Eliaz, D., Solomonov, A. & Shimanovich, U. Microcompartmentalization controls silk feedstock rheology. *Langmuir* **39**, 8984–8995 (2023).
111. Kwak, H. W., Ju, J. E., Shin, M., Holland, C. & Lee, K. H. Sericin promotes fibroin silk I stabilization across a phase-separation. *Biomacromolecules* **18**, 2343–2349 (2017).
112. Malay, A. D., Oktaviani, N. A., Chen, J. & Numata, K. Spider silk: rapid, bottom-up self-assembly of MaSp1 into hierarchically structured fibers through biomimetic processing. *Adv. Funct. Mater.* **35**, 2408175 (2025).
113. Lemetti, L. et al. Molecular crowding facilitates assembly of spidroin-like proteins through phase separation. *Eur. Polym. J.* **112**, 539–546 (2019).
114. Laity, P. R. & Holland, C. The rheology behind stress-induced solidification in native silk feedstocks. *Int. J. Mol. Sci.* **17**, 1812 (2016).
115. Holland, C., Terry, A., Porter, D. & Vollrath, F. Comparing the rheology of native spider and silkworm spinning dope. *Nat. Mater.* **5**, 870–874 (2006).
116. Sparkes, J. & Holland, C. The rheological properties of native sericin. *Acta Biomater.* **69**, 234–242 (2018).
117. Laity, P. R., Baldwin, E. & Holland, C. Changes in silk feedstock rheology during cocoon construction: the role of calcium and potassium ions. *Macromol. Biosci.* **19**, 1800188 (2019).
118. Shim, J.-K. & Lee, K.-Y. Chilling results in failure of silk secretion by wandering larvae of Plodia interpunctella. *J. Asia Pac. Entomol.* **18**, 483–487 (2015).
119. Blackledge, T. A. & Hayashi, C. Y. Silken toolkits: biomechanics of silk fibers spun by the orb web spider *Argiope argentata* (Fabricius 1775). *J. Exp. Biol.* **209**, 2452–2461 (2006).
120. Yoshioka, T., Tsubota, T., Tashiro, K., Jouraku, A. & Kameda, T. A study of the extraordinarily strong and tough silk produced by bagworms. *Nat. Commun.* **10**, 1469 (2019).
121. Agnarsson, I., Kuntner, M. & Blackledge, T. A. Bioprospecting finds the toughest biological material: extraordinary silk from a giant riverine orb spider. *PLoS ONE* **5**, e11234 (2010).

122. Yazawa, K., Nakayama, K. & Gotoh, Y. Silkworm cocoon waste revitalization: regenerated fibers using higher-molecular-weight fibroin achieve high strength and toughness. *ACS Sustain. Chem. Eng.* **11**, 2151–2159 (2023).
123. Blake, R. W. & Domenici, P. *Biomechanics in Animal Behaviour*. (Garland Science, 2021).
124. Li, C. et al. Regenerated silk materials for functionalized silk orthopedic devices by mimicking natural processing. *Biomaterials* **110**, 24–33 (2016).
125. Magaz, A. et al. Porous, aligned, and biomimetic fibers of regenerated silk fibroin produced by solution blow spinning. *Biomacromolecules* **19**, 4542–4553 (2018).
126. Ling, S. et al. Polymorphic regenerated silk fibers assembled through bioinspired spinning. *Nat. Commun.* **8**, 1387 (2017).
127. Madani, G., Lamping, E. & Cannon, R. Engineering a cysteine-deficient functional *Candida albicans* Cdr1 molecule reveals a conserved region at the cytosolic apex of ABCG transporters important for correct folding and trafficking of Cdr1. *mSphere* **6**, e01318–e01320 (2021).
128. Huang, Y. et al. Detecting protein−protein interaction during liquid −liquid phase separation using fluorogenic protein sensors. *Mol. Biol. Cell* **35**, ar41 (2024).
129. Inoue, S. et al. Silk fibroin of *Bombyx mori* is secreted, assembling a high molecular mass elementary unit consisting of H-chain, L-chain, and P25, with a 6:6:1 molar ratio. *J. Biol. Chem.* **275**, 40517–40528 (2000).
130. Whaite, A., Wang, T., Macdonald, J. & Cummins, S. Major ampullate silk gland transcriptomes and fibre proteomes of the golden orb-weavers, *Nephila plumipes* and *Nephila pilipes* (Araneae: Nephilidae). *PLoS ONE* **13**, e0204243 (2018).
131. Lu, Y. et al. Complete sequences of the velvet worm slime proteins reveal that slime formation is enabled by disulfide bonds and intrinsically disordered regions. *Adv. Sci.* **9**, 2201444 (2022).
132. Wöltje, M., Isenberg, K. L., Cherif, C. & Aibibu, D. Continuous wet spinning of regenerated silk fibers from spinning dopes containing 4% fibroin protein. *Int. J. Mol. Sci.* **24**, 13492 (2023).
133. Ishida, H. et al. Artifact-free preparation of biological samples for SEM by optimized water freeze-drying. *Sci. Rep.* **16**, 717 (2025).
134. Santos, S., Barcons, V., Christenson, H. K., Font, J. & Thomson, N. H. The intrinsic resolution limit in the atomic force microscope: implications for heights of nano-scale features. *PLoS ONE* **6**, e23821 (2011).
135. Wan, Q. et al. Carbon nanotubes facilitate silk hierarchical assembly by dry drawing. *Small Struct.* **5**, 2300435 (2024).
136. Song, K., Zhang, H., Zhang, X., Li, Y. & Zhu, P. Cryo-ET comparison of the hierarchical ultrastructure of silkworm, spider, and artificial silk fibers. *Nat. Commun.* **17**, 3608 (2026).
137. Roldán, D., Redenbach, C., Schladitz, K., Kübel, C. & Schlabach, S. Image quality evaluation for FIB-SEM images. *J. Microsc.* **293**, 98–117 (2024).
138. Wu, A. S. et al. Carbon nanotube fibers as torsion sensors. *Appl. Phys. Lett.* **100**, 201908 (2012).
139. Esmaeili, M. et al. Ptychographic X-ray tomography of silk fiber hydration. *Macromolecules* **46**, 434–439 (2013).
140. Perera, D., Li, L., Walsh, C., Wang, Q. & Schniepp, H. C. Natural spider silk nanofibrils produced by assembling molecules or disassembling fibers. *Acta Biomater.* **168**, 323–332 (2023).

Acknowledgements

This work was supported by the Engineering and Physical Sciences Research Council [grant number EP/X015416/1]. For the purpose of open access, the author has applied a Creative Commons Attribution (CC BY) licence to any Author Accepted Manuscript version arising.

Author contributions

M.Z. and C.H. conceptualized the review. M.Z. drafted the manuscript, collected the data and prepared the figures. All authors contributed equally intellectually and reviewed the manuscript.

Competing interests

The authors declare no competing interests.

Additional information

Supplementary information The online version contains Supplementary material available at https://doi.org/10.1038/s43246-026-01232-8.

Correspondence and requests for materials should be addressed to Martin Zaki or Benjamin J. Allardyce.

Peer review information *Communications Materials* thanks Michael Woltje and the other anonymous reviewer(s) for their contribution to the peer review of this work. A peer review file is available.

Reprints and permissions information is available at http://www.nature.com/reprints

Publisher's note Springer Nature remains neutral with regard to jurisdictional claims in published maps and institutional affiliations.

Open Access This article is licensed under a Creative Commons Attribution 4.0 International License, which permits use, sharing, adaptation, distribution and reproduction in any medium or format, as long as you give appropriate credit to the original author(s) and the source, provide a link to the Creative Commons licence, and indicate if changes were made. The images or other third party material in this article are included in the article's Creative Commons licence, unless indicated otherwise in a credit line to the material. If material is not included in the article's Creative Commons licence and your intended use is not permitted by statutory regulation or exceeds the permitted use, you will need to obtain permission directly from the copyright holder. To view a copy of this licence, visit http://creativecommons.org/licenses/by/4.0/.

© The Author(s) 2026